Haptic Simulation of Needle-tissue Interaction Based on Shape Matching

Yuan Tian†, Yin Yang‡, Xiaohu Guo†, Balakrishnan Prabhakaran†
†University of Texas at Dallas
800 W Campbell Road
Richardson, TX 75080 USA
{yxt114020, suraj, xguo, praba}@utdallas.edu
‡University of New Mexico
1 University Blvd NE
Albuquerque, NM 87131 USA
yyang@ece.unm.edu

***Abstract*—Simulating needle-tissue interaction in a haptic-enabled environment is an essential component in many virtual surgical training procedures, where the trainee would practice needle insertion and retraction repeatedly. Efficiency and stability are of major importance for the corresponding visual and haptic rendering. In this paper, we present a novel system for a real-time and robust simulation of needle-tissue interaction with haptic devices. The soft tissue is modeled using the classic shape matching method for its excellent numerical stability. It can interact with a one dimensional inextensible rigid/flexible virtual needle freely. The feedback force from the needle is formulated as the gradient of the potential energy of the soft tissue based on particle constraint. Under the framework of shape matching, the feedback force can be efficiently evaluated and smoothly rendered through haptic devices. Our model can also support various material properties so that tissues of different stiffness can be well handled.**

***Keywords*—haptic rendering; virtual reality; needle insertion; shape matching;**

I. Introduction

Needle insertion is an important approach for investigating the patient's physical condition. It plays an essential role in many medical and clinic treatments such as injections, neurosurgery, biopsies, and brachytherapy cancer treatment [1]. Physicians and clinical students typically practice the needle insertion operations on animal bodies or even on real patients. This is a long-term training procedure, since it is difficult to steer a flexible needle to reach the target in a specific placement accurately, while avoiding other bony anatomical structures. Furthermore, in some applications like percutaneous procedure, organs are very close to each other, to the order of millimeters. As a result, extra training of needle insertion is required to minimize unnecessary piercing damages or disease spreading. Modern surgical training and planning systems favor computer based simulator in the virtual reality (VR) environment, which is free of risks to patient's safety. The trainee could experience realistic visual feedbacks such as the tissue deformation and needle deflection. Compared to traditional training, improved surgical skills with minimized costs are reported in previous works [2], [3], [4] in terms of increased action accuracy and reduced procedure time. For a better training result, many studies introduce haptic devices into surgical simulations [5], [6], [7], which leads to a more comprehensive user experience. The haptic-enabled VR allows the user to manipulate the needle to interact virtual tissue models while feeling the interaction torques and forces.

There are three major concerns must be taken into account when a haptic-enabled needle-tissue simulation system is designed namely, the computational efficiency, system stability and physical realism. Since the haptic device typically requires high-frequency update rate (e.g., over 1KHz) to ensure the smoothness of the force rendering, the underlying simulation algorithm must be sufficiently fast to avoid jittery feedback forces. If a bursting movement is applied to the haptic handle by the user, as the acceleration approaches infinity, an impulse-like interaction force would arise and could potentially crash the background simulation. Consequently, the simulation system is expected to be able to provide robust feedbacks under such "abnormal" user inputs. The simulated tissue deformation and needle deflection need to be physically plausible as well so that a realistic visual impression can be delivered to the user. The corresponding feedback force should reflect the motion trajectory of the virtual haptic interface point (HIP) in a physically reasonable way. Such collision/contact between the virtual needle and deformable tissue imposes extra difficulties as many physical interactions need to be processed simultaneously.

Inspired by these challenges, we introduce a novel needle-tissue interaction model in this paper. The shape matching (SM) method [8] is employed to simulate the soft tissue. This method excels in its concise formulation and lightweight implementation efforts, in comparison with widely-used finite element modes, while still yielding visually plausible deformation results. More importantly SM holds an unconditionally stable time integration scheme, which makes the simulator very robust under unexpected user inputs. We propose a novel constraint particle coupling method to efficiently couple the needle and soft tissue. Constraint particles are inserted into SM clusters along the needle's path and the corresponding needle movement serves as the *target position* to trigger the SM deformation. The tissue-needle force is evaluated as the gradient of the potential energy of the associated SM clusters so that the internal force is always on the direction minimizing the deformation and renders realistic user feedback.

The rest of paper is organized as follows: Section II briefly reviews some existing related work. Section III gives an overview of our method. In Section IV, our SM based needle insertion model is explained. Section V details how to compute the force feedback for the haptic device. Section VI shows the

978-1-4799-5964-8/14/$31.00 ©2014 IEEE

experiments results using our interaction model. Conclusion and potential future work are discussed in Section VII.

II. Related Work

Simulating needle-tissue interaction has been an active topic in recent years [1]. There exists a wide range of methods modeling the dynamic behavior of the soft tissue such as mass-spring system [9], chain-mail model [10] or meshless discretization [11]. A large volume of contributions are developed based on the finite element method (FEM) [12], [13], [14] for deformable simulation. This method is built upon a well-established numerical theory and yields accurate simulation results. However, FEM is relatively computationally expensive especially when the mesh holds a large number of degrees of freedom. Another drawback lies in the fact that the FEM always requires a well conditioned system matrix, which may not be always available if certain elements are badly degenerated or flipped under extreme user manipulations. Although we may still be able to proceed the simulation with more sophisticated numerical treatments such as invertible element [15], it significantly slows down the simulation performance and is rarely used in a real surgical simulation.

There are also quite a few variations of the needle model for example, the rigid needle [16], [9], the flexible symmetric-tip needle [17], as well as the bevel-tip needle [18]. Chentanez *et al* [13] simulated the flexible rod based on the *Cosserat theory* [19]. DiMaio and Salcudean [20] simulated needle using FEM with geometric nonlinearity. This method was extended to 3D using 4-node tetrahedral elements by Goksel *et al* [21]. The needle-tissue interaction model is more involved as it includes various physical mechanisms. Most existing work deals with such interaction as a natural lateral constraint [17], [13] within the framework of FEM. Goksel *et al* [21] applied the local remeshing and recomputed the regional stiffness matrix for an updated local discretization so that a tissue node always coincided with the needle tip. Alternatively, different meshes can be tied together by binding constraints [22], [23]. However this approach could potentially distribute the needle force over other nearby tissue nodes. Therefore, the largest deformation at the tissue is not consistent with the needle.

Orthogonal to the aforementioned contributions, we present a tissue simulator based on the shape matching method [8], a pseudo-physics based approach. In SM, the deformable solid is discretized by a group of particle clusters. Particles trend to move towards their goal positions, computed as the best-matching rigid body transformation for a particle cluster, to minimize the deformation. The stability and the efficiency can be further improved with some proper numerical augments [24], [25], making SM well suited for real-time haptic-enable simulation. The needle is modeled as a series of rigid rod element connected using angular springs [26]. This model can be considered as an extended version of mass-spring system. Unlike FEM elastic rod model [20], the springs contain only angular degrees of freedom and the length of the needle is automatically preserved. We extend our earlier work [27], which handles the interaction between HIP and the deformable objects, by adding multiple constraint particles along the needle's path for the needle-tissue coupling. Our method does not need expensive remeshing process and the resulting contact force can be easily evaluated for haptic rendering.

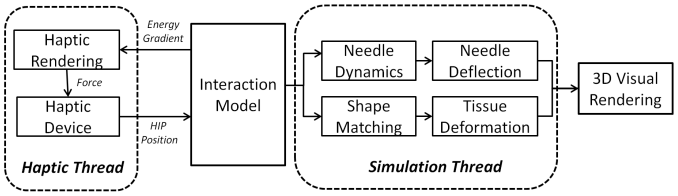

Fig. 1. An overview of our multi-rate haptic-enabled needle insertion simulation framework.

III. System Overview

We applied a multi-rate framework similar to the one proposed in [27]. Fig. 1 outlines a general overview of the proposed system. Simulation thread calculates the needle deflection and tissue deformation *asynchronously*. Haptic thread inputs the HIP position to our interaction model, computes the force feedback and sets force and torque of the haptic device.

SM method is a particle based method. Ill-structure organ meshes, such as meshes with holes, dangling edges, isolated triangles/vertices or even polygon soup without any connection information can be conveniently handled in our framework. The underlying representation of the soft tissue is generated using a cube or voxel mesh generated by applying voxelization over the input mesh structure using squashing cube method [28]. Each cube represents a SM cluster. The deformation is calculated based on cube mesh first and the embedded surface mesh will be updated by barycentric interpolation. The deflectable yet inextensible needle is modeled by spring-connected rigid rods [26]. At each simulation step when the updated HIP position is passed to the interaction model, the geometries of both soft tissue as well as the defected needle is computed. The feedback force is evaluated as energy gradient and passed back to hatpic device for force rendering.

IV. SM based Needle-tissue Interaction Model

In this section, we briefly review the SM method as well as the constraint particle method for needle-tissue coupling. We will also introduce the algorithmic variations at different stages of needle interaction and adjustment of the material parameter.

In our system, a SM cluster is a voxel or cube with eight particles at its corners. Each particle is associated with a *mass*, an *initial position*, a *current position* as well as a *goal position* which are denoted with $m_i, \mathbf{x}_i^0, \mathbf{x}_i$ and $\mathbf{g}_i$ respectively. At each time step, each particle trends to moved towards its goal positron. Since a particle could be shared by multiple clusters, the current position of one particle is set as the average from all of its associated clusters. To find the goal positions, SM computes the optimal rotation $\mathbf{R}$ and translation $\mathbf{t}$ for each cluster. We refer the reader to the related document [8] for a detailed derivation of $\mathbf{R}$ and $\mathbf{t}$. The system deformation energy E is computed as the summation of square deviations between the current position and goal position for all the particles:

$$E = \sum_i m_i \mid \mathbf{R}\mathbf{x}_i^0 + \mathbf{t} - \mathbf{x}_i \mid^2 = \sum_i m_i \mid \mathbf{g}_i - \mathbf{x}_i \mid^2 . \qquad (1)$$

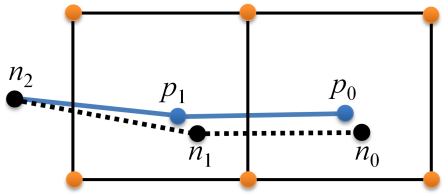

Fig. 2. An illustrative 2D example of the constraint particle mechanism used in our system. The square boxes are the particle clusters. All particles sit at the corners of the square shown as orange dots. When the needle (shown as the black dash line) penetrate into the tissue, two extra constraint particles p_0 and p_1 (shown as black dots), are inserted into the clusters. These constraint particles trigger the shape matching deformation. Accordingly, the needle is deflected to the new position (solid blue line).

A. Constraint Particle

In order to evaluate the feedback forces, we need to make sure that whenever the needle gets into the tissue, it always hits some particles so that the follow up SM simulation for the soft tissue could be triggered. Therefore we add extra constraint particles (CP) into the interfacing cluster (e.g., the cluster at which the needle-tissue interaction occurs).

This strategy well complements our previous method, constraint particle coupling (CPC) for 3-DOF haptic simulation of with SM based deformable model [27]. In CPC, only a single CP is added to the interfacing cluster as long as a collision between the HIP and the deformable object is detected. The newly-inserted CP increases the system energy and deforms the object. On the other hand, there are many different possible interactions between the needle and the soft tissue such as puncture, deep insertion or retraction in the scenario of needle-tissue interaction. This indicates that the needle does not only interact the tissue at its tip (where the HIP sits) but also at all of the other positions across needle's body. Coupling using only a single particle as in CPC is not sufficient to well model various needle dynamics. Consequently, we regularly sample the needle along its body and each sampling leads to a CP added into the cluster. In other words, CPs are inserted into the clusters along the path of the needle's trajectory. Similar to CPC method, some ghost particles (GP) are added into the cluster to retain the optimal translation $\mathbf{t}$ and rotation $\mathbf{R}$. Fig. 2 shows an 2D example for CP. Needle is modeled as a composite of interconnected rigid rods of unit length. Every two adjacency rods are connected with a angular spring [20]. The haptic device directly manipulates the needle in 3D and the needle is rendered in 3D environment (proxy) by including all the inserted CPs, which is shown as solid blue line in Fig. 2.

B. Puncturing

Puncturing refers to making a shallow hole on the outer layer of a tissue using the needle tip. In the puncturing step, collision detection locates the interaction point between needle and tissue based on a pre-built hierarchical sphere tree for the tissue mesh. The algorithm for puncturing step is as following:

1) We add the first CP p_0 at the interaction position on the tissue surface and set its current position as the position of needle tip node n_0.

2) Perform shape matching.

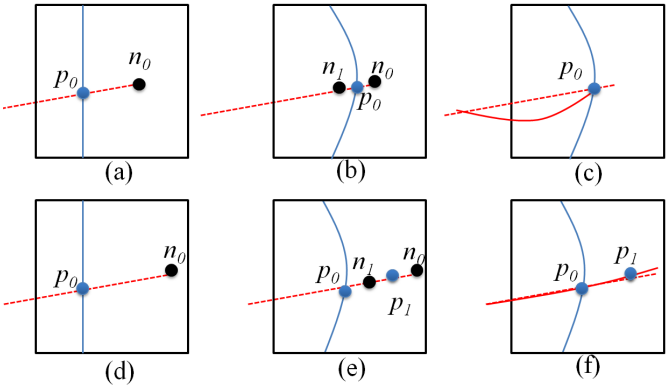

Fig. 3. Two different scenarios are shown for puncturing steps. The black square is a cluster. Blue line represents the surface of the tissue. The red line is the needle proxy and the red dash line is the needle finger. (a)(b)(c) illustrate the scenario for pre-puncture, (d)(e)(f) illustrate that the needle punctures the tissue model. (a) A CP p_0 is added at the interaction point. (b) shape matching is performed to deform the tissue, the successive node after tip node n_1 is outside the tissue, therefore tissue cannot be punctured. (c) Needle deflection is computed by the current configuration. (d) A CP p_0 is added at the interaction point. (e) The successive node n_1 is inside the tissue, therefore tissue is punctured and a new CP p_1 is added one sampling unit from p_0 along the needle. Now p_0 is associated with n_1, and p_1 is with n_0. (f) Needle deflection is computed by the current configuration.

3) Check if the successive node on the needle is inside the tissue. If inside, the tissue is punctured by the needle, a new CP is added one sampling unit away from the first CP. For the next time step, the tip node is associated with the newly added CP, and the first CP is with the successive node.

4) Needle deflection is computed by curve dynamics.

To better illustrate this algorithm, two scenarios for puncturing are shown in Fig. 3.

C. Insertion/Retraction

After puncturing step, the needle is either pushed or pulled during training procedure. The rigid needle as well as symmetric tip flexible needle will pierce straightly into the inner layer. For beveled tip needle, we simulate the needle deflection by adding a displacement δ which is tangential to the needle tip direction. The user could then rotate the needle shaft to steer the insertion direction. During insertion, rest part of needle will follow the path of needle tip inside the tissue, which are recorded by all the CPs in our model. While retraction, the needle will also follow the path. Therefore, we propose the following algorithm:

1) At current time step, based on the user operation of needle (rotate, push, or pull), compute the new configuration of the needle.

2) Based on the needle configuration and relations between CP and needle nodes, set current positions of CPs as positions of needle nodes, and perform shape matching for tissue deformation.

3) Adjust the relations between the CPs and needle nodes; If the needle node is now before the corresponding CP, re-associate this CP with the nearest needle node before this CP; if the needle is

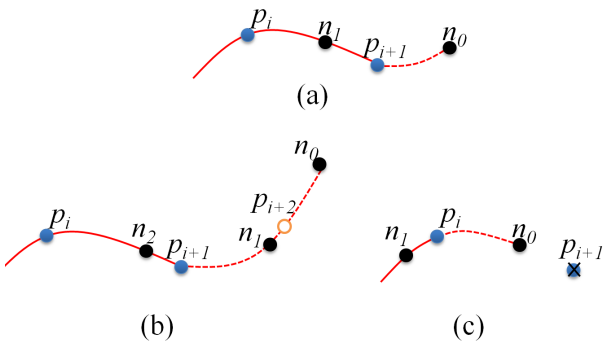

Fig. 4. Needle insertion and needle retraction. (a) is a needle path with p_i and p_{i+1}. (b) needle insertion, needle tip node n_0 does not have corresponding CP, then a new CP p_{i+2} is added. (c) needle retraction, CP p_{i+1} does not have corresponding node, then p_{i+1} is removed from the cluster.

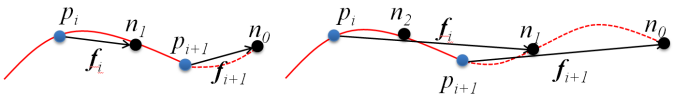

Fig. 5. Force computation for sticking and slipping friction. Left represents the sticking force, since the needle proxy keep attached with the tissue; right describes the slipping force, where there exists relative motion between the needle and the tissue.

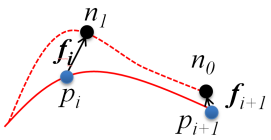

Fig. 6. Force computation for clamping. Since the needle finger moves in perpendicular direction of the needle shaft, the corresponding CP can compute the clamping force.

after the needle node, re-associate this CP with the nearest needle node after this CP.

4) Add/remove CP. After step(3), if there is a CP which does not have corresponding needle node, then remove this CP. If there is a needle node which does have corresponding CP, then add a CP one unit away from its successive CP.

Fig. 4 illustrates the insertion and retraction procedure of the interaction model.

V. Haptic Rendering

As shown in Eq. 1, each CP added into the whole system will influence the elastic potential energy. Similar with [27], the force can be naturally computed as the derivative with respect to $\mathbf{x}_i$, the current position of each CP:

$$f = m_i(\mathbf{x}_i - \mathbf{g}_i) = m_i(\mathbf{x}_i - \mathbf{R}\mathbf{x}_i^0 + \mathbf{T}). \quad (2)$$

Since the energy describes the elasticity of the whole SM system, this force is the internal force caused by particle motion.

Since Eq.2 is another important contribution, we would like to emphasize that this contribution is non-trivial. The force is physically reasonable and coincide with the interaction between needle and tissue. Previous work categorizes the interaction force as stiffness force, friction force, cutting force, and clamping force. Our contact force model could describe all these forces.

Stiffness force belongs to the pre-puncture stage in our interaction model, and it corresponds to the vector from the proxy needle tip to the finger needle tip. When the force vector is beyond one unit, the needle has punctured the tissue, which coincides with a large deformation of tissue caused by needle pushing.

Friction force during insertion or retraction is a form of stick-slip friction. The magnitude of the friction depends on the difference between the velocity of the needle and the tissue. Sticking means the location of some tissue part is attached to the needle, while slipping means the movement of tissue is constrained to be parallel to the needle shaft. Fig. 2 shows the force computation for two scenarios using our interaction model.

Clamping force is generated due to the resistance offered by the tissue when the needle moves in the direction perpendicular to the needle shaft. The scenario is showed in Fig.6.

VI. Results

In this section, we describe the experiment results using our needle-tissue interaction model. The results show the realistic and stable simulation of tissue deformation, and the accurate haptic rendering for different physical phenomena. All experiments are performed on a machine with a dual Intel Xeon 2.8 GHz CPU, 6GB memory, ATI FirePro 2260 card and Windows 7 64bit OS. We use a Geomagic Touch 3 DOF haptic device to steer the virtual needle and experience the force feedback. Chai3d library [29] is used to develop the 3D environment. Under the framework as introduced in Sec. III, the haptic thread can maintain a high update frequency as 1 KHz, while keeping the fps of 3D rendering as around 27.6.

Fig. 7 shows the 3D environment for needle-tissue interaction. A flexible needle is inserted into the liver surface model. Constraint Particles are added along the needle path for coupling. As shown in left image of Fig. 7, cube mesh which covers the liver model has deformation caused by needle insertion.

Another experiment is performed to evaluate the visual performance for different phases of the needle interaction with tissue. As shown in Fig. 8, the interaction model can simulate different stages of needle-tissue interaction such as

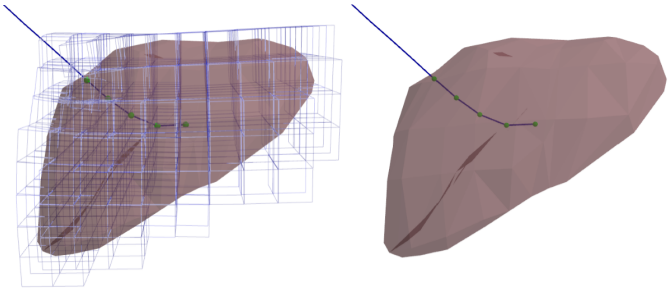

Fig. 7. A flexible needle is inserted into the liver mesh. Left image shows the deformation of red cube mesh. Right shows the needle deflection and added Constraint Particles which are represented by green spheres.

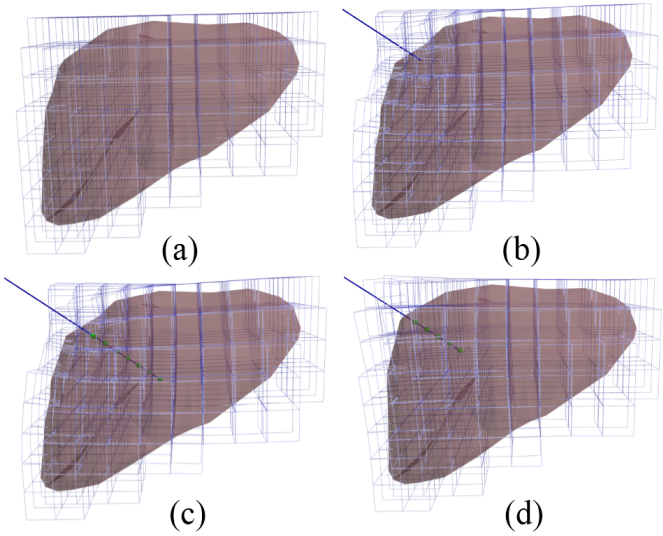

Fig. 8. Snapshots of the haptic simulation of needle insertion with a rigid needle. From left to right, the snapshots show the puncture stage, the insertion stage, and the retraction stage.

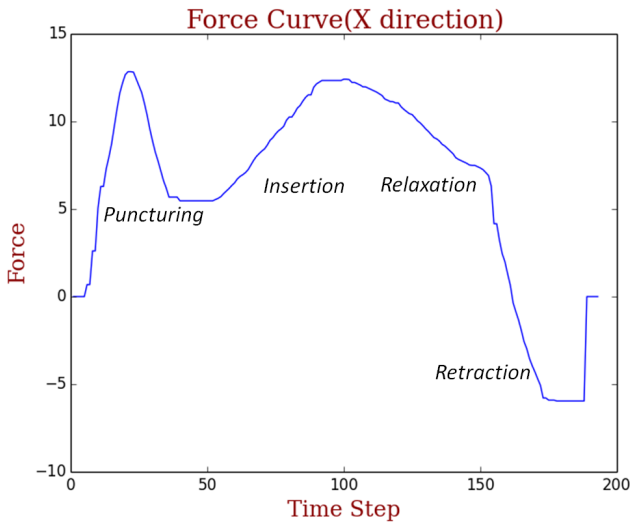

Fig. 9. Force feedback while probe the needle only in X direction. The needle interactions includes puncturing, insertion, relaxation and retraction, fit very well with the force feedback.

puncturing, insertion, and retraction. In different phases, our model will perform the deformation of cube mesh firstly, and then interpolate the surface mesh of the liver.

To evaluate the force feedback, we have performed an experiment in which the needle is inserted through the liver tissue model. The effects of insertion are studied over a single dimension (in this case, along the x-axis). In this experiment, we apply needle to puncture the tissue, and insert into deep region of tissue, then the needle is retracted from the tissue until the needle is totally outside. As shown in Fig. 9, our haptic rendering method generates corresponding force feedback for different phases. When the needle punctures the tissue, force reduces sharply after a force peak. Then, the slipping friction force increases with the penetration. When the needle insertion slows down, it comes to a relaxation stage, and the friction force is formed by both slipping and sticking force. For retraction, the force also increases because of friction force, and finally when needle is totally outside, the force returns to zero. This force curve is similar with the measurement results in [30].

The beveled-tip flexible needle is very important since the user could steer this kind of needle by rotating the needle base to avoid the bones or other organs before the target. We show an experiment which is similar to previous work [23], [13]. Fig. 10 shows a real-time flexible needle steering to avoid two cube obstacles inside the tissue model. Tissue deformations are complex because of the heterogeneous, nonlinear, elastic and viscous behavior of soft tissue. We can manually set the particle stiffness (mass) of different layer. During the insertion of flexible needle, it will have the large deflection with an increase of the stiffness.

For more details, the demo video can be downloaded at http://www.utdallas.edu/~yxt114020/needleSimulation.mp4.

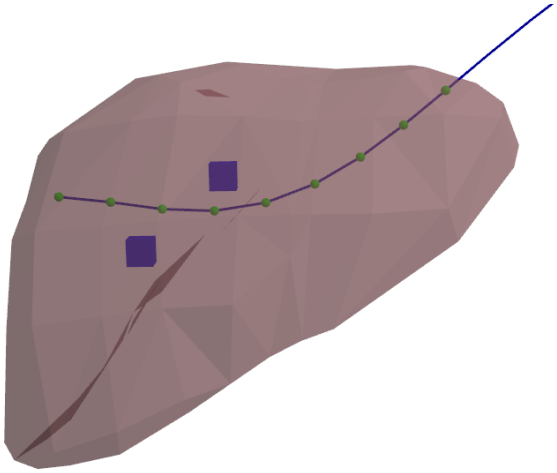

Fig. 10. An example showing the beveled tip flexible needle steering to avoid two cubes obstacles. The user rotate the needle base to change the direction of needle bending.

VII. Conclusion

In this paper, we have demonstrated the interest of using SM method to simulate the tissue model for medical training. We have also presented a needle-tissue interaction model for coupling the needle movement and tissue deformation. Our model provides a fast and stable haptic simulation for needle insertion training, and allows the user to build a more complex 3D environment with a more complicated heterogeneous tissue.

In the future, we will perform experiments for certain real-world clinical procedures involving needle insertion, to validate the accuracy of our model. We would like to extend our work to surgical needle suturing applications together with thread simulation. Moreover, for some needle insertion applications, the needle shaft cannot be simplified to a unidimensional rod. Our interaction model aims to add only

one contact particle along the needle path. Scenarios with distributed contacts between needle shaft and tissue model would be investigated in the future.

ACKNOWLEDGMENT

This material is based upon work supported by the National Science Foundation under Grant No. 1012975. Any opinions, findings, and conclusions or recommendations expressed in this material are those of the author(s) and do not necessarily reflect the views of the National Science Foundation.

REFERENCES

[1] N. Abolhassani, R. Patel, and M. Moallem, "Needle insertion into soft tissue: A survey," *Medical engineering & physics*, vol. 29, no. 4, pp. 413–431, 2007.

[2] A. G. Gallagher, E. M. Ritter, H. Champion, G. Higgins, M. P. Fried, G. Moses, C. D. Smith, and R. M. Satava, "Virtual reality simulation for the operating room: proficiency-based training as a paradigm shift in surgical skills training," *Annals of surgery*, vol. 241, no. 2, p. 364, 2005.

[3] R. M. Satava, "Identification and reduction of surgical error using simulation," *Minimally Invasive Therapy & Allied Technologies*, vol. 14, no. 4-5, pp. 257–261, 2005.

[4] N. E. Seymour, A. G. Gallagher, S. A. Roman, M. K. O?Brien, V. K. Bansal, D. K. Andersen, and R. M. Satava, "Virtual reality training improves operating room performance: results of a randomized, double-blinded study," *Annals of surgery*, vol. 236, no. 4, p. 458, 2002.

[5] S. Ullrich and T. Kuhlen, "Haptic palpation for medical simulation in virtual environments," *IEEE Transactions on Visualization and Computer Graphics*, vol. 18, no. 4, pp. 617–625, 2012.

[6] C. Basdogan, S. De, J. Kim, M. Muniyandi, H. Kim, and M. Srinivasan, "Haptics in minimally invasive surgical simulation and training," *Computer Graphics and Applications, IEEE*, vol. 24, no. 2, pp. 56–64, March 2004.

[7] P. Wang, A. Becker, I. Jones, A. Glover, S. Benford, C. Greenhalgh, and M. Vloeberghs, "Virtual reality simulation of surgery with haptic feedback based on the boundary element method," *Computers and Structures*, vol. 85, no. 78, pp. 331 – 339, 2007. [Online]. Available: http://www.sciencedirect.com/science/article/pii/S0045794906003920

[8] M. Müller, B. Heidelberger, M. Teschner, and M. Gross, "Meshless deformations based on shape matching," ser. SIGGRAPH '05, pp. 471–478.

[9] M. Marchal, E. Promayon, J. Troccaz *et al.*, "Simulating prostate surgical procedures with a discrete soft tissue model," in *Proceedings of 3rd Workshop in Virtual Reality Interactions and Physical SImulation*, 2006.

[10] F. P. Vidal, N. W. John, A. E. Healey, and D. A. Gould, "Simulation of ultrasound guided needle puncture using patient specific data with 3d textures and volume haptics," *Computer Animation and Virtual Worlds*, vol. 19, no. 2, pp. 111–127, 2008.

[11] J. Xu, L. Wang, K. Wong, and P. Shi, "A meshless framework for bevel-tip flexible needle insertion through soft tissue," in *Biomedical Robotics and Biomechatronics (BioRob), 2010 3rd IEEE RAS and EMBS International Conference on*, Sept 2010, pp. 753–758.

[12] H. Kataoka, S. Noda, H. Yokota, S. Takagi, R. Himeno, and S. Okazawa, "Simulations of needle insertion by using a eulerian hydrocode fem and the experimental validations," in *Medical Image Computing and Computer-Assisted Intervention MICCAI 2008*, ser. Lecture Notes in Computer Science, D. Metaxas, L. Axel, G. Fichtinger, and G. Szkely, Eds. Springer Berlin Heidelberg, 2008, vol. 5242, pp. 560–568.

[13] N. Chentanez, R. Alterovitz, D. Ritchie, L. Cho, K. K. Hauser, K. Goldberg, J. R. Shewchuk, and J. F. O?brien, "Interactive simulation of surgical needle insertion and steering," in *in ACM SIGGRAPH*, 2009.

[14] O. Goksel, K. Sapchuk, and S. E. Salcudean, "Haptic simulation of needle and probe interaction with tissue for prostate brachytherapy training," in *World Haptics Conference (WHC), 2011 IEEE*. IEEE, 2011, pp. 7–12.

[15] G. Irving, J. Teran, and R. Fedkiw, "Invertible finite elements for robust simulation of large deformation," in *Proceedings of the 2004 ACM SIGGRAPH/Eurographics Symposium on Computer Animation*, ser. SCA '04. Aire-la-Ville, Switzerland, Switzerland: Eurographics Association, 2004, pp. 131–140.

[16] J. Westwood *et al.*, "Simulating needle insertion and radioactive seed implantation for prostate brachytherapy," *Medicine Meets Virtual Reality 11: NextMed: Health Horizon*, vol. 94, p. 19, 2003.

[17] S. P. DiMaio and S. Salcudean, "Needle steering and motion planning in soft tissues," *Biomedical Engineering, IEEE Transactions on*, vol. 52, no. 6, pp. 965–974, 2005.

[18] R. Alterovitz, K. Goldberg, and A. Okamura, "Planning for steerable bevel-tip needle insertion through 2d soft tissue with obstacles," in *Robotics and Automation, 2005. ICRA 2005. Proceedings of the 2005 IEEE International Conference on*. IEEE, 2005, pp. 1640–1645.

[19] M. Bergou, M. Wardetzky, S. Robinson, B. Audoly, and E. Grinspun, "Discrete elastic rods," *ACM Transactions on Graphics (TOG)*, vol. 27, no. 3, p. 63, 2008.

[20] S. P. DiMaio, "Modelling, simulation and planning of needle motion in soft tissues," Ph.D. dissertation, Citeseer, 2003.

[21] O. Goksel, S. E. Salcudean, and S. P. Dimaio, "3d simulation of needle-tissue interaction with application to prostate brachytherapy," *Computer Aided Surgery*, vol. 11, no. 6, pp. 279–288, 2006.

[22] E. Sifakis, T. Shinar, G. Irving, and R. Fedkiw, "Hybrid simulation of deformable solids," in *Proceedings of the 2007 ACM SIGGRAPH/Eurographics symposium on Computer animation*. Eurographics Association, 2007, pp. 81–90.

[23] C. Duriez, C. Guébert, M. Marchal, S. Cotin, and L. Grisoni, "Interactive simulation of flexible needle insertions based on constraint models," in *Medical Image Computing and Computer-Assisted Intervention–MICCAI 2009*. Springer, 2009, pp. 291–299.

[24] A. R. Rivers and D. L. James, "FastLSM: fast lattice shape matching for robust real-time deformation," in *SIGGRAPH '07*.

[25] M. Müller and N. Chentanez, "Solid simulation with oriented particles," *ACM Trans. Graph.*, vol. 30, no. 4, pp. 92:1–92:10, Jul. 2011.

[26] O. Goksel, E. Dehghan, and S. E. Salcudean, "Modeling and simulation of flexible needles," *Medical engineering & physics*, vol. 31, no. 9, pp. 1069–1078, 2009.

[27] Y. Tian, Y. Yang, X. Guo, and B. Prabhakaran, "Haptic-enabled interactive rendering of deformable objects based on shape matching," in *Haptic Audio Visual Environments and Games (HAVE), 2013 IEEE International Symposium on*. IEEE, 2013, pp. 75–80.

[28] D. L. James, J. Barbič, and C. D. Twigg, "Squashing cubes: Automating deformable model construction for graphics," in *ACM SIGGRAPH 2004 Sketches*, ser. SIGGRAPH '04. New York, NY, USA: ACM, 2004, pp. 38–. [Online]. Available: http://doi.acm.org/10.1145/1186223.1186271

[29] F. Conti, D. Morris, F. Barbagli, and C. Sewell, "Chai 3d," *Online: http://www. chai3d. org*, 2006.

[30] E. Dehghan, X. Wen, R. Zahiri-Azar, M. Marchal, and S. E. Salcudean, "Needle-tissue interaction modeling using ultrasound-based motion estimation: Phantom study," *Computer Aided Surgery*, vol. 13, no. 5, pp. 265–280, 2008.